Earthquakes and Structures, *Vol. 18, No. 1 (2020) 113-127*
DOI: https://doi.org/10.12989/eas.2020.18.1.113

Experimental evaluation of external beam-column joints reinforced by deformed and plain bar

Mahdi Adibi *[1], Jalil Shafaei [2a] and Fatemeh Aliakbari[1]

[1]School of Civil Engineering, College of Engineering, University of Bojnord, Iran
[2]Faculty of Civil Engineering, Shahrood university of technology, Iran

(*Received January 30, 2018, Revised September 1, 2019, Accepted September 13, 2019*)

Abstract. In this study, the behavior of external beam-column joints reinforced by plain and deformed bars with non-seismic reinforcement details is investigated and compared. The beam-column joints represented in this study include a benchmark specimen by seismic details in accordance with ACI 318M-11 requirements and four other deficient specimens. The main defects of the non-seismic beam–column joints included use of plain bar, absence of transverse steel hoops, and the anchorage condition of longitudinal reinforcements. The experimental results indicate that using of plain bars in non-seismic beam-column joints has significantly affected the failure modes. The main failure mode of the non-seismic beam-column joints reinforced by deformed bars was the accumulation of shear cracks in the joint region, while the failure mode of the non-seismic beam-column joints reinforced by plain bars was deep cracks at the joint face and intersection of beam and column and there was only miner diagonal shear cracking at the joint region. In the other way, use of plain bars for reinforcing concrete can cause the behavior of the substructure to be controlled by slip of the beam longitudinal bars. The experimental results show that the ductility of non-seismic beam-column joints reinforced by plain bars has not decreased compared to the beam-column joints reinforced by deformed bars due to lack of mechanical interlock between plain bars and concrete. Also it can be seen a little increase in ductility of substructure due to existence of hooks at the end of the development length of the bars.

Keywords: external RC beam-column joints; plain bars; deformed bars

1. Introduction

Beam–column joints in reinforced concrete (RC) moment frames are key components to guarantee integrity and overall stability when the frame is subjected to seismic loading (Park and Paulay 1975, Paulay and Priestley 1992), and post-earthquake surveys of damaged RC structures have demonstrated that, in many cases, damage to RC moment frames was concentrated in the beam–column joints, contributing to partial or total collapse of the structure (De Risi *et al*. 2016, Fernandes *et al*. 2013, Moehle and Mahin 1991, Miller 1998, Sezen *et al*. 2003-2000, Doğangün 2004, Ghobarah *et al*. 2006, Gur *et al*. 2009, Zhao *et al*. 2009, Kam *et al*. 2011). In other words, among different elements, the beam-column joints have been highly susceptible to seismic excitations and the failure of joint panel has been frequently observed (Khan *et al*. 2018, Del Vecchio *et al*. 2014, Sezen *et al*. 2003-2000, Park *et al*. 1995a,b, Sezen *et al*. 2000a,b , Hall *et al*. 1996, Uang *et al*.1999, ATC 1989, Hakuto 1995, Priestley and MacRae 1996). Furthermore, it has been observed that due to discontinuity of structural geometry and inferior confinement conditions, external beam–column joints are more vulnerable to seismic loading than are internal beam–column joints (Paulay and Priestley 1992, Moehle and Mahin 1991, Miller 1998, Sezen *et al*. 2003a, b, Doğangün 2004, Ghobarah *et al*. 2006, Gur *et al*. 2009, Zhao *et al*. 2009). Many reinforced concrete structures were designed and constructed before the development of seismic codes or according to earlier versions of seismic codes, and these structures have significant deficiencies in the beam–column joint regions due to the absence of transverse reinforcement and insufficient bond length of the beam bottom bars (Engindeniz *et al*. 2005). Beam–column joints in such existing structures may fail prior to the formation of plastic hinges in the beams framing into that joint. Performance of these connections are also negatively affected by the quality of the bond between concrete and plain bars. Mo and Chan (1996) have shown experimentally that the bond strength of plain rebars was only 28.6% that of deformed rebars; the slip at failure was greater for the plain rebars than for the deformed rebars; and increasing the concrete compressive strength was able to improve the bond properties (Mo and Chan 1996, Verderame *et al*. 2009, Masi *et al*. 2008-2009). In another experimental study on bond behavior between plain reinforcing bars and concrete, Xing *et al* (2015) concluded that the bond stress experienced by plain bars is quite lower than that of the deformed bars given equal structural characteristics and details. In average, plain bars appeared to develop only 18.3% of the bond stress of deformed bars. Also, the influence of bond and shear effect on the behavior of beam-column joint is discussed in some numerical studies (Lowes and Altoontash, JSE 2003;

*Corresponding author, Assistant Professor
E-mail: m.adibi@ub.ac.ir, mahdi.adibi@gmail.com
[a]Assistant Professor
E-mail: jshafaei@shahroodut.ac.ir

ISSN: 2092-7614 (Print), 2092-7622 (Online)

Youssef and Ghobarah, JEE 2001).

In RC structures reinforced by plain bars the behavior of the joints is different from those reinforced by deformed bars. That is, the mode of slippage of the steel bars commonly governs failure of the joint and diagonal shear failure is less influential (Calvi *et al*. 2002, Liu and park 2000-2001, Bedirhanoglu *et al*. 2010, Russo and Pauletta, 2012, Braga *et al*. 2009). Different experimental studies (Pampanin *et al*. 2002, Calvi *et al*. 2002) on joints reinforced by plain bars have shown that low shear capacity of panel zone prevents formation of flexural plastic hinge in beams. In addition, early sliding of plain bars, especially in beams, prevents a beam to reach its ideal flexural capacity, and this prevents shear cracking to form in the joint.

Adibi *et al*. (2017a, b) investigated the behavior of non-seismically detailed external beam–column joints of existing concrete structures reinforced by plain bars and proposed a retrofit method to protect the joint region against earthquake. Experimental results demonstrated a relatively large pinching in the hysteresis response of the joint specimens. The authors concluded that the pinching may be attributed primarily to sliding of the smooth bars and shear failure in the joint region.

Shafaei *et al*. (2014) studied the effects of joint flexibility on lateral response of reinforced concrete frames. The beam-column joints investigated in this study reinforced by deformed bars and represented non-seismic beam column joints detailing with some shear strength deficiencies in the term of absence of transverse steel hoops in the joint panel zone and insufficient beam bottom bar development length in the joint panel zone. Based on experimental results, the author concluded that the average ductility for the non-seismically detailed specimens decreased by 27% and 54% with respect to the seismically detailed specimen and pinching of the hysteretic curve for the non-seismically detailed specimens was significantly increased.

In this study, five beam-column joints included joints reinforced by plain and deformed bars were selected and experimental behavior of seismically and non-seismically detailed external beam–column joints of existing concrete structures are examined and compared. By this research, difference of damaged modes and crack mechanism of joints reinforced by plain and deformed bars clearly were shown. In addition, some important seismic parameters such as strength, stiffness, ductility and energy dissipation capacity of substructure have been investigated.

2. Experimental program

External beam–column joints represented in this study are considered to be isolated from RC building built prior to the 1970s (Taylor *et al*. 1925, Duhman 1953, Pernot 1945, Barker 1967, Edvard and Tanner 1996). External beam–column joints are selected because they are more vulnerable than internal joints due to seismic load. The experimental program consists of reversed cyclic quasi-static unidirectional loading of five half-scaled external RC beam–column joints. Two units are tested as-built to serve as beam–column joints reinforced by plain bars, and three units are tested as-built to serve as beam–column joints reinforced by deformed bars. The nomenclature used for various specimens is presented in Table 1.

Table 1 Schedule of test specimens

Spc	$\frac{P}{A_g f'_c}$	Bar Type	Col		Beam		
			ρ_{col}(%)	Av/s(mm)	ρ_{top}(%)	ρ_{bot}(%)	Av/s(mm)
JRD1	0.15	DB[b]	2	1.66	1.2	0.9	1.66
JRD2	0.15	DB	2	1.66	1.2	0.9	1.66
JRD3	0.15	DB	2	1.66	1.2	0.9	1.66
JRP1[a]	0.07	PB[c]	1	0.41	0.6	0.4	0.59
JRP2[a]	0.15	PB	1	0.41	0.6	0.4	0.59

[a] The anchorage length of the beam longitudinal bars is almost equal to the joint effective width with 180 degree hooks at the ends of the bars.
[b] Deformed Bar
[c] Plain Bars
A_g: gross sectional area
f'_c: standard cylinder compressive strength of concrete
A_v: cross-sectional area of each stirrup
s: spacing of stirrups
ρ: longitudinal reinforcement ratio

Table 2 Compressive strength of concrete for different specimens

Specimen	Compressive Strength (MPa)
JRD1	23.0
JRD2	23.3
JRD3	24.7
JRP1	23.6
JRP2	22.5

Table 3 Mechanical properties of reinforcement bars

Bar type		Position	f_y	f_u	e_y	e_u
			(MPa)		(%)	
Deformed Bar	F8	Stirrup	350	410	0.18	18.0
	F14	Longitudinal Bars	460	680	0.20	13.0
Plain Bar	F5.5	Beam Stirrup	340	470	0.12	28.0
	F6.5	Column Stirrup	224	336	0.13	25.0
	F12.0	Beam Longitudinal Bars*	360	500	0.15	28.5
	14.0	Column Longitudinal Bars	320	450	0.17	30.0

2.1 Material properties

All test specimens were constructed using normal weight and ready mixed concrete. Table 2 shows the concrete strength on the day of testing for the five specimens. Mechanical properties of the steel reinforcement used in the specimens are shown in Table 3.

2.2 Test specimens

A total of five specimens were investigated in this study.

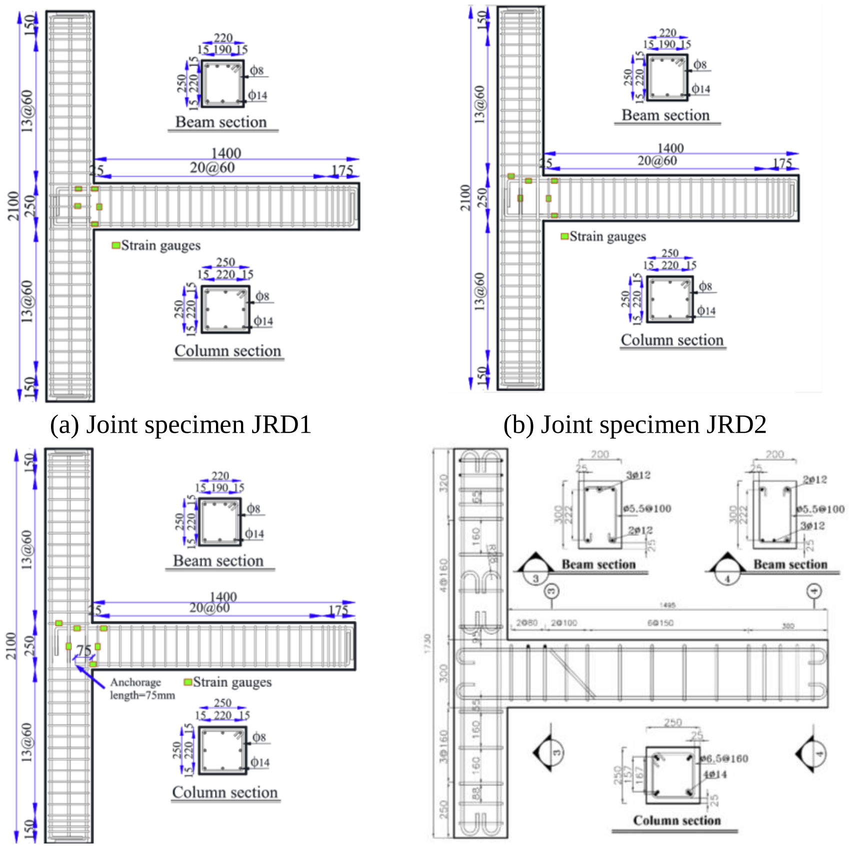

(a) Joint specimen JRD1 (b) Joint specimen JRD2

(c) Joint specimen JRD3 (d) Joint specimen JRP1 and JRP2

Fig. 1 Dimensions and reinforcement details of jointsspecimens (dimensions in millimeters)

JRD1, JRD2 and JRD3 were joints reinforced by deformed bars, and JRP1 and JRP2 were joints reinforced by plain bars. Specimen JRD1 represented a seismic beam–column joint designed to satisfy ACI 318M-11 requirements (2005), whereas specimens JRD2 and JRD3 had inadequate reinforcement detailing in the joint region and represented RC structural sub-assembly having deficient detailing. Specimen JRD1 had sufficient shear reinforcement and anchorage length of the beam longitudinal reinforcement in the joint region, satisfying the requirements of ACI 318M-11 (2005) for the design of beam–column joints in RC structure as shown in Fig. 1(a). The column height and the beam length represented the distance to the points of contraflexure for seismic bending moments. The transverse reinforcement in the column was Φ8 deformed bars with 135° end hooks that were spaced at 60 mm inside and outside the joint panel zone. The transverse reinforcement of the beam was Φ8 rectangular ties starting at 25 mm from the face of the column that were spaced at 60 mm for the beam length. The longitudinal and transverse reinforcement for the beam, column and joint satisfied ACI 318M-11 seismic requirements (2005). The dimensions and reinforcement details of specimen JRD1 are shown in Fig. 1(a). Specimens JRD2 and JRD3 represented deficiently-detailed external RC beam–column joint specimens, with similar dimensions and reinforcement details to specimen JRD1, except for the transverse reinforcement of the column and the anchorage condition of the beam bottom longitudinal reinforcement in the joint region that did not satisfy seismic requirements. Specimen JRD2 was designed as a shear-deficient specimen provided with no transverse shear reinforcement in the joint region and specimen JRD3 was designed as a shear-deficient and anchorage critical specimen with the bottom longitudinal reinforcement in the beam anchored 75 mm far from the column face and with no transverse reinforcement installed in the joint region. The non-seismic specimens were expected to fail by joint shear and pullout of beam bottom bars before a plastic hinge formed in the beam. The dimensions and reinforcement details of the deficient specimens JRD2 and JRD3 are shown in Fig. 1(b) and 1(c), respectively.

Specimens JRP1 and JRP2 represented beam column joints reinforced by plain bars. The main defects of these non-seismic beam–column joints include use of plain bar, absence of transverse steel hoops, and the anchorage condition of longitudinal reinforcements. The anchorage length of the beam bars is almost equal to the joint effective width with 180-degree hooks at the ends of the bars. Characteristics of these two joint specimens are similar and only the level of axial loads to the respected columns are as much as 7% and 15% of the section capacity ($A_g f_c'$) for specimens JRP1 and JRP2, respectively. The details of these specimens are shown in Fig. 1(d).

2.3 Test setup and loading protocol

For all of the joint specimens tested in this study, a constant axial load was applied to the column. The axial

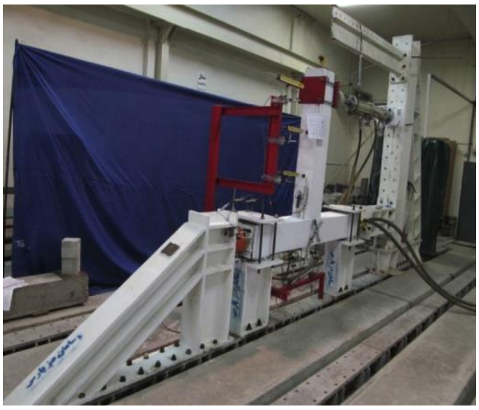

(a) View of the test

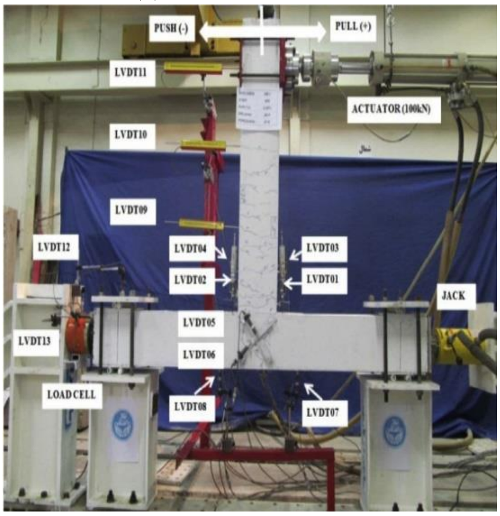

(b) Instrumentation detail

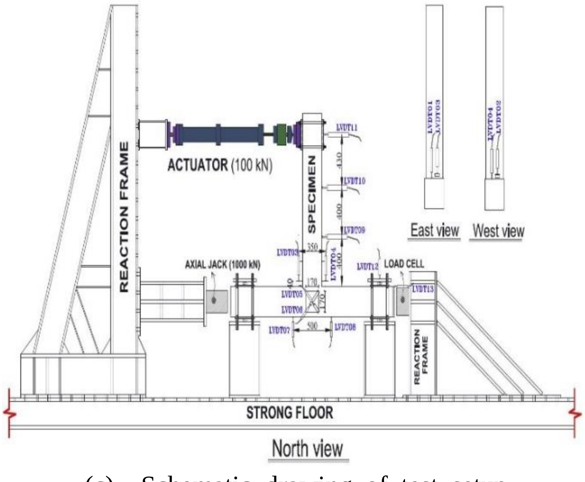

(c) Schematic drawing of test setup

Fig. 2 Overview of test setup and instrumentation

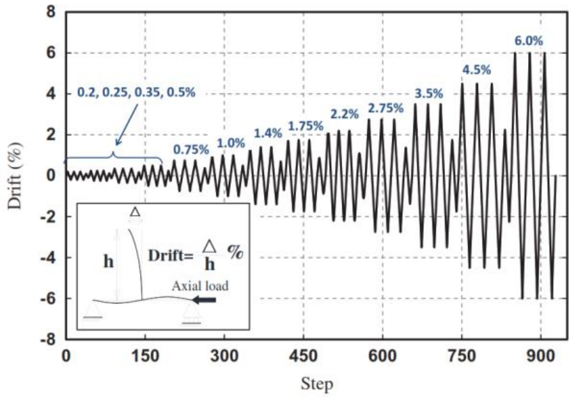

Fig. 3 Lateral cyclic loading protocol

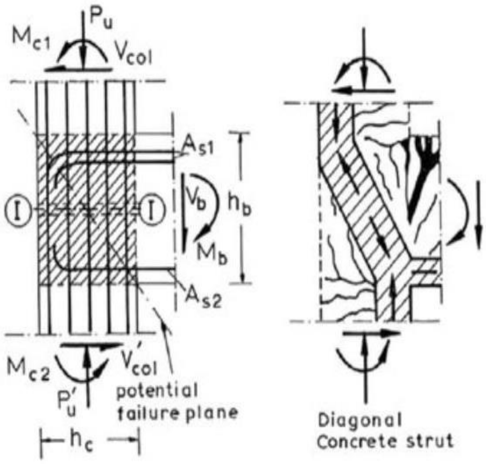

(a) strut & tie

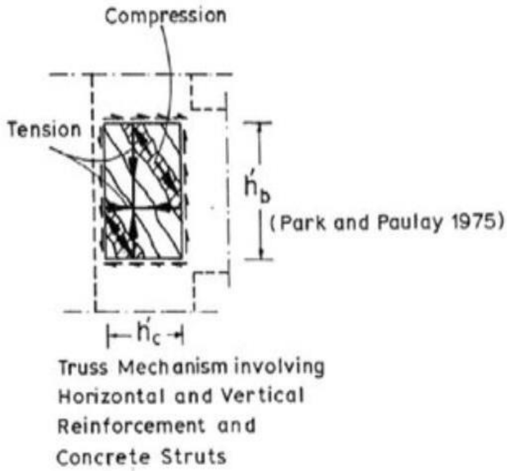

(b) Trus mechanism

Fig. 4 Mechanisms of internal forces in the joint region (Paulay and Priestley 1992, Tsonos and Stylianidis 2002)

load was applied in a force-controlled mode and was maintained constant throughout each test. For joint specimens reinforced by plain bars, two levels of axial load representing the story level were applied to the column: $0.07f'c \times b \times h$, and $0.15f'c \times b \times h$, where b and h are the width and depth of the cross section of the column and P is the axial load. After application of axial load to the column, low rate lateral cyclic loading of increasing amplitudes was applied at the end of the beam in a displacement-controlled mode. The loading procedure for all specimens was based on criteria specified in ACI 374.1-05 (2005). The lateral cyclic loading protocol used for the specimens is shown in Fig. 3. For each specimen a total of 10 electrical resistance strain gauges were attached to longitudinal and transverse reinforcement at critical locations to record the magnitude of reinforcement strains that developed at different loading stages, and 13 linear variable displacement transducers

Drift=±1.0% Drift=±1.75% Drift=±3.5%

Fig. 5 Damage progression and crack observation for specimen JRD1

(LVDTs) were used to record the beam rotation, column rotation and joint distortion, as shown in Fig. 2(b). A microcomputer controlled data acquisition system was used to record the data from strain-gauges, LVDTs and load cells. Positive and negative loading directions and the hydraulic jacks are indicated in Fig. 2(b). Schematic drawing of the test setup is shown in Fig. 2(c).

3. Test observations

Mechanism of internal forces in the joint region was shown in Fig. 4. According to this figure, the mechanism of shear force transfer in the joint is divided into truss and strut & tie mechanisms. In the joints without any transverse reinforcement in the joint region, the truss mechanism is naturally absent, and the strut & tie mechanism contribute alone to the entire shear force transfer. Generally, shear cracking is expected to occur in the joint region in these connections (Figs. 5-10), but as shown in Figs. 11-14, in joint specimens reinforced by plain bars, cracking pattern was appeared differently.

3.1 Specimen JRD1

The performance of the seismic control specimen (JRD1) represented the desired target performance of the beam–column joints reinforced by deformed bars when designed using current seismic code provisions. The axial load of $0.15f'c\times b\times h$ (b and h are the width and depth of the cross section of the column) was applied to the sub-structure in this connection. The damage pattern of specimen JRD1 is shown in Figs. 5 and 6, illustrating that specimen JRD1 failed by flexural yielding in the beam with moderately ductile performance. The first flexural cracks appeared at the bottom of the beam at 0.25% drift and gradually propagated to a length of 750 mm. First yield of the beam longitudinal reinforcement occurring at a drift ratio of 1.1%. Spalling of concrete cover at the column surface commenced at a drift ratio between 1.75% and 2.2%, and diagonal cracking in the joint zone began at a drift of 1.75% for the push direction. Additional cracking in the joint panel zone appeared thereafter as loading progressed, but crack widths remained fine throughout the test. At a drift ratio of 3.5% the beam became extensively cracked along a distance equal to its depth from the column face, and at a drift ratio of 4.5% wide cracks developed in the beam potential plastic hinge zone and rubble started falling, as shown in Fig. 5. The test was terminated at a drift ratio of 6.0% and at the end of the test, the joint panel zone remained unchanged except for the presence of the fine cracks, with no recorded loss of column axial load. Mechanism of crack development in the joint area is shown in Fig. 6.

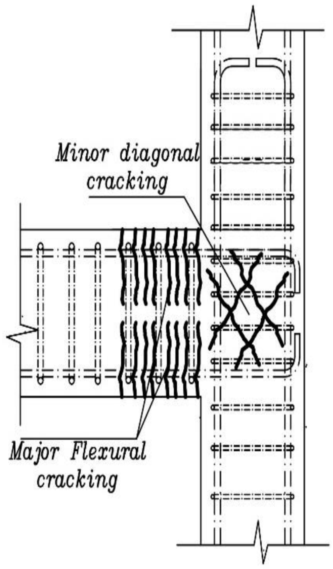

Fig. 6 Mechanism of cracks development for specimen JRD1

3.2 Specimen JRD2

The joint specimen JRD2 reinforced by deformed bars and had no transverse shear reinforcement in the joint region. The axial load of 0.15f'c×b×h (b and h are the width and depth of the cross section of the column) was applied to the sub-structure in this connection.

The first flexural cracks of specimen JRD2 formed as for specimen JRD1, but X-shape cracks in the joint panel zone commenced at a drift ratio of 0.75%, indicating imminent joint failure. The flexural and diagonal cracks grew in size and number as the drift ratio increased. Spalling of concrete cover appeared in the joint region at a drift ratio of between 1.4% and 2.0%, and from a drift of 2.0%, the cracking was mainly concentrated in the joint region and formed a typical X-shaped pattern, as shown in Fig. 7. At a drift ratio of 3.5% the concrete in the joint panel

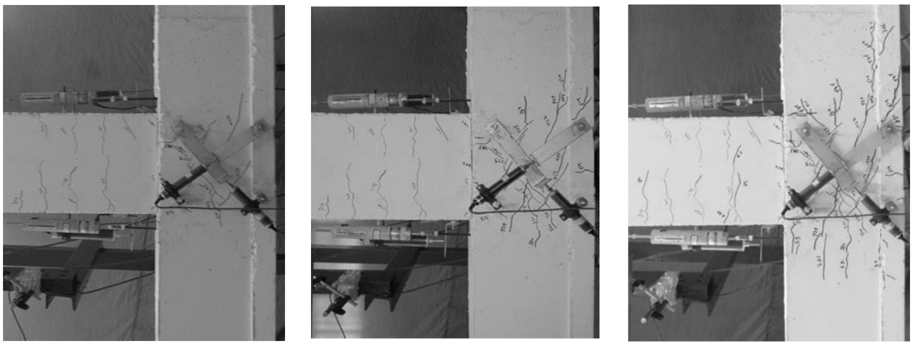

Drift=±1.0% Drift=±1.75% Drift=±3.5%

Fig. 7 Damage progression and crack observation for specimen JRD2

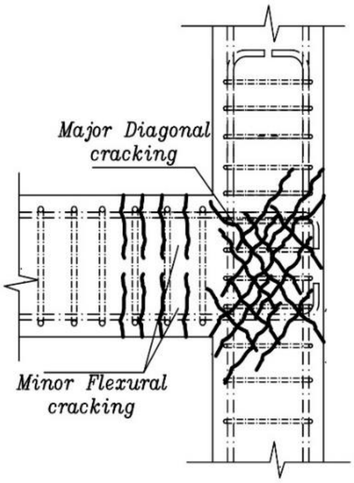

Fig. 8 Mechanism of cracks development for specime nJRD2

zone spalled and crushed off and exposing the column longitudinal reinforcement. Yield of beam longitudinal reinforcement was not recorded throughout the test. The absence of adequate column ties in the joint region caused the compressive failure of the diagonal struts and this phenomenon can be clearly seen from the failure pattern of specimen JRD2, as shown in Fig. 7. The progress of damage to specimen JRD2 during successive displacement steps is illustrated in Fig. 7. Also, mechanism of crack development in the joint area is shown in Fig. 8.

3.3 Specimen JRD3

The joint specimen JRD3, is a joint specimen reinforced by deformed bars with non-seismic details, like specimen JRD2. But, in specimen JRD3, the bottom longitudinal reinforcement of the beam developed until 75 mm far from the column face (Fig. 1). Also, any transverse reinforcement in the joint region was not seen in this specimen like the joint specimen JRD2. The axial load of $0.15f'c\times b\times h$ was applied to the sub-structure. The progress of damage to specimen JRD3 during successive displacement steps is illustrated in Fig. 9. The first flexural cracks of specimen JRD3 were observed at the column face at a drift ratio of 0.25% and gradually propagated to a length of 300 mm for the pull direction, and to 650 mm for the push direction. The vertical cracks in the joint panel formed at a drift ratio of 0.5%, due to bond-slip of the beam bottom reinforcement for the pull direction, and diagonal shear cracks in the joint zone developed at a drift ratio of 0.75% for the push direction. The beam reinforcement pulled out due to bond failure at approximately 2/3 of their yield stress and yield of the beam longitudinal reinforcement was not recorded throughout the test. When repeating the same displacement cycle, the beam reached the target displacement but at lower load level and the beam reinforcement started to slip out of the joint zone, with an associated reduction in the developed strain in the reinforcement.

When the specimen was next loaded to right, the bond-slip cracks opened and the lateral load-carrying capacity

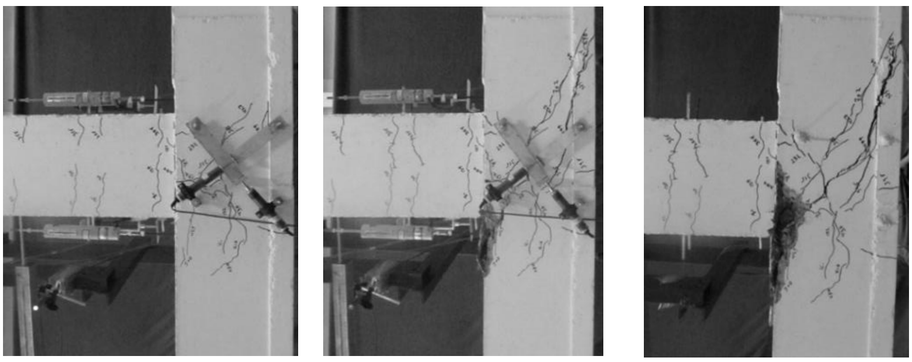

Drift=±1.0% Drift=±1.75% Drift=±3.5%

Fig. 9 Damage progression and crack observation forspecimen JRD3

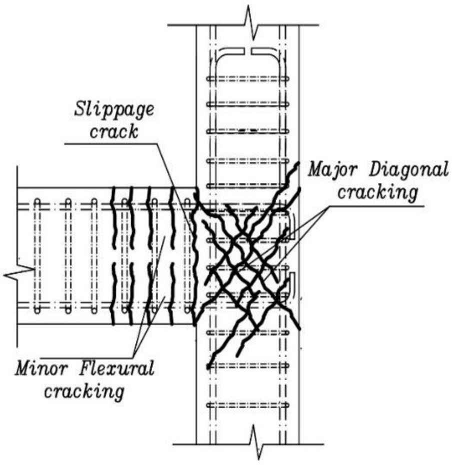

Fig. 10 Mechanism of cracks development for specimen JRD3

deteriorated significantly, and then when reversed back to the left the diagonal shear cracks in the joint panel zone opened, causing crushing of the concrete, deterioration of the bond condition of the beam bottom reinforcement.

A 10% reduction in the column axial load was recorded during the last cycles due to joint shear failure. Fig. 9 illustrates the crack patterns and damage progress during the test at different drift ratios. Mechanism of crack development in the joint area is shown in Fig. 10.

3.4 Specimen JRP1

The joint specimen JRP1 reinforced by plain bars. This specimen has some defects such as absence of transverse steel hoops, and the anchorage condition of longitudinal reinforcements. The axial load of $0.07f'c \times b \times h$ was applied to the sub-structure in this connection. Development of flexural cracks of specimen JRP1 at different stages during test are illustrated in Fig. 11. The first cracks formed at a drift ratio of 0.45% at two locations of the beam: at a distance of 37 cm far from the column face and at the intersection of beam with column. After that, additional flexural cracks appeared over the zone where longitudinal bars were bent. During elastic behavior, the joint and the column did not undergo any cracking. At a drift ratio of 1.35%, the crack pattern did not vary significantly, instead, rocking behavior governed the response and spalling of concrete cover at the joint region appeared. At a drift ratio of 1.8%, longitudinal cracks parallel to longitudinal bars developed over the beam. In addition, diagonal cracks in the joint panel zone commenced at this drift ratio. At a drift ratio of 2.7%, concrete wedge spalling at the exterior face of the joint was observed. At a drift ratio of 3.65%, X-shape cracks in the joint panel is formed and concrete wedge spalled and crushed off. Mechanism of crack development in the joint area is shown in Fig. 12. As shown in these figures, damage modes of substructure include deep and wide crack at the face of the column and diagonal cracking in the panel zone of the joint. An important observation is delay in forming of diagonal cracks until a drift ratio of 1.8%. Diagonal cracking in the joint region was seen in the same ratio in the specimen designed using current seismic code provisions (specimen JRD1).

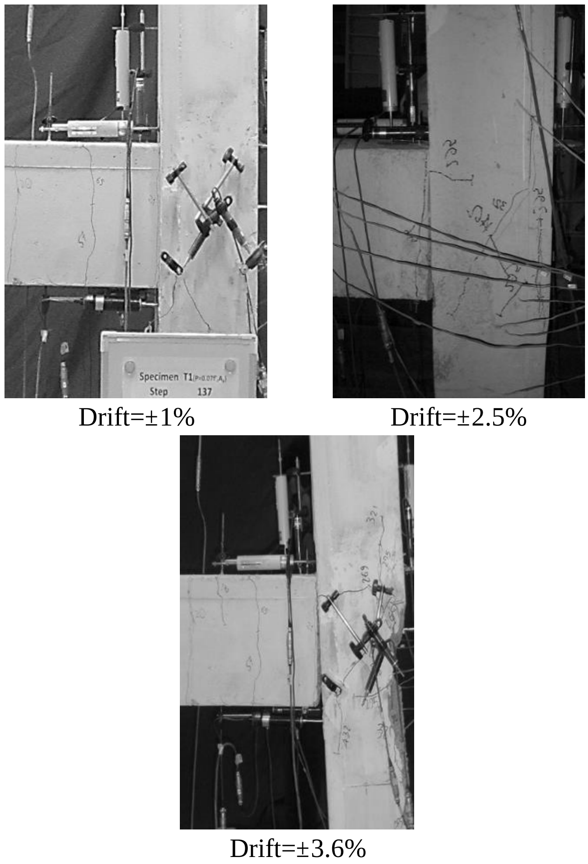

Fig. 11 Damage progression and crack observation for specimen JRP1

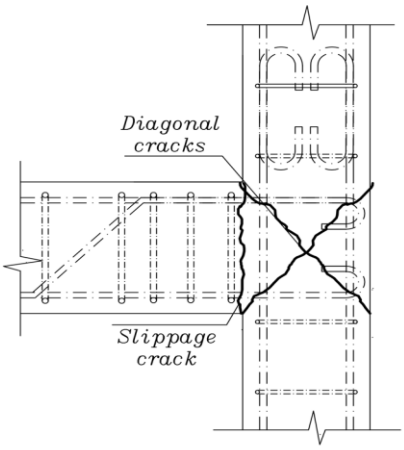

Fig. 12 Mechanism of cracks development in the joint region for specimen JRP2

3.5 Specimen JRP2

The joint specimen JRP2 reinforced by plain bars and its properties is like the joint specimen JRP1. The axial load of $0.15f'c \times b \times h$ was applied to the sub-structure in this connection which is similar to the axial load in the joint specimens reinforced by deformed bars.

Drift=±1% Drift=±2.5% Drift=±4.5%

Fig. 13 Damage progression and crack extension of specimen JRP2

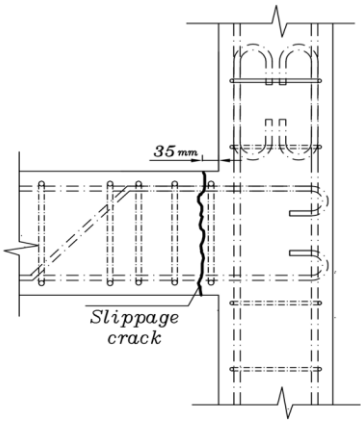

Fig. 14 Mechanism of cracks development in the joint region for specimen JRP2

Fig. 13 illustrates development of flexural cracks of specimen JRP2 at different stages. The first cracks formed at a drift ratio of 0.45% at two locations of the beam: at a distance of 37 cm and 3.5 cm far from the column face. At drift ratio of 1.8%, width of intersectional crack grew up and reached 5.5 mm, and spalling of concrete cover at bottom of the beam appeared at a drift ratio of 2.7%. At a drift ratio of 3.65%, longitudinal cracks parallel to longitudinal bars developed over the beam in the joint region and spalling of concrete cover commenced at back face of the column. Any diagonal cracks in the joint panel zone was not seen in this specimen. Mechanism of crack development in the joint zone is shown in Fig. 14. As shown in this figure, failure mechanism in this substructure is restricted to deep and wide crack at the face of the column and any diagonal cracking is not seen in the panel zone. This may be related to higher axial load and more confinement of the panel zone relative to specimen JRP1.

4. Experimental results and discussion

In the present section, based on the various experimental results of specimens, effect of type of the reinforcing bars (deformed and plain bars) in beam–column joint was investigated. Also, seismic parameters such as ductility, strength, stiffness and energy dissipation capacity of the substructures were evaluated.

4.1 Hysteretic response of specimens

Force–displacement hysteretic response during cyclic loading is the most important characteristic for assessing the seismic performance of a structural component, as this characteristic indicates both the energy dissipation efficiency and the ductility capacity of the component (Park and Paulay 1975, Paulay and Priestley 1992). Therefore, force–displacement hysteretic response of joint specimens is shown in Fig. 15 in the form of horizontal load applied to the top of the beam versus corresponding drift ratio. The important points during the tests are annotated based on the test observations in the represented hysteretic response of joints specimens. Also, predicted flexural strength of the specimen calculated from the beam nominal moment capacity (Mn) is indicated by horizontal dashed lines. Different failure modes of substructures can be find out from the represented hysteretic response of specimens. Also, the differences between the behavior of concrete connections reinforced by plain and deformed bars are characterized by comparing the hysteretic curves and failure modes.

Specimen JRD1 exhibited ductile force–displacement hysteretic response with no notable pinching or strength drops by the end of testing (see Fig. 15(a)). This appropriate performance attributed to the adequate shear reinforcement and anchorage length of the beam longitudinal reinforcement in the joint region, satisfying the requirements of ACI 318M-11 (2005) for the design of beam–column joints in RC structure. As shown in Figs. 5, 6 and 15(a), occurrence of plastic hinge is clearly visible at the the end of the beam due to yielding of the longitudinal reinforcements, corresponded to 32 kN and 41.5 kN lateral load in pull and push direction, receptively. The cracking in the panel zone of the joint is insignificant.

The hysteretic loops of the non-seismic specimens (JRD2 and JRD3) show considerable pinching and continuous stiffness degradation with increasing displacement with respect to the seismic specimen (JRD1), which is primarily attributed to the joint shear failure of specimen JRD2 (see Fig. 15(b)) and joint shear failure and bond failure of the beam bottom reinforcement of specimen JRD3 (see Fig. 15(c)). As shown in Figs. 7, 8, and 15(b), yielding of the longitudinal bars and forming of plastic hinge were not seen in the specimen JRD2, which is reinforced by deformed bars and without any transverse steel hoops in the joint region. The dominant damage mode inducing to the substructure and cause to drop off the load bearing of the substructure is the formation of the diagonal cracking in the panel zone of the joint. Different damage modes were seen in the joint specimen JRD3, which has lack of transverse shear reinforcement in addition to reducing development length of the longitudinal bars of the beam. The main damage mode of this joint specimen was deep crack at the face of the column due to debounding and slipage of the bars throughout the concrete in the joint region. Also, diagonal cracking in the joint panel zone was seen in the specimen due to lack of transverse shear reinforcement.

The specimen JRP1 underwent axial load to columns as much as 7% of the section capacity ($A_g f_c'$). The relationship between drift and lateral force of specimen JRP1 is shown in Fig. 15(d). The curve shows relatively high pinching effect and degradation of strength with increasing displacement. The pinching may be attributed primarily to sliding of the smooth bars and shear failure in the joint region. Pattern of crack and damage to the specimen is a few wide cracks that have divided the beam into a few solid segments, and this has caused rocking fluctuation of the segments under cyclic action. As shown in Figs. 7 and 11, damage modes in the joint specimens reinforced by plain and deformed bars (specimen JRP1 and JRD2) are different despite of similarity of deficiency in both of joint specimens. Diagonal cracking in the joint region is seen in the joint reinforced by deformed bars and is the main damage mode of the substructure, but in the joint reinforced by plain bars, diagonal cracking in the joint region is not seen and the main damage mode is the deep slipage crack at the intersection of the beam and column. Also, some of the longitudinal bars of the beam in joint reinforced by plain bars has reached to the yielding tensile stress in spite of large slipage due to existence of 180° end hooks at the end of development length of the bars. Thus, the joint specimen reinforced by plain bars reached its nominal flexural strength (corresponding to 15.8 kN lateral force) in pull direction which strength of weak face of the beam controls bearing capacity of the substructure.

In push direction (strong face of the beam), the specimen did not develop full nominal flexural strength and reached 17 kN lateral load that was only 0.81% of its nominal capacity (21 kN). The strain-gages on top longitudinal bars recorded a maximum strain of $0.80\varepsilon_y$ during the test. Overall, the smooth bars have prevented the beam to reach its full nominal sectional strength. The joint specimen JRP2 underwent axial load to columns as much as 15% of the section capacity ($A_g f_c'$). The relationship between drift and lateral force of specimen JRP2 is shown in Fig. 15(e). The curve shows relatively high pinching effect and relatively more rapid decline of strength with increasing displacement compared to the specimen JRP1. An increase of 50% of flexural strength of the beam is seen in pull direction in comparison with JRP1. The strain-gages recorded 3200 μs on bottom longitudinal bars of the beam that indicates post yield strength of the bars. In push direction (strong face of the beam), the specimen did not

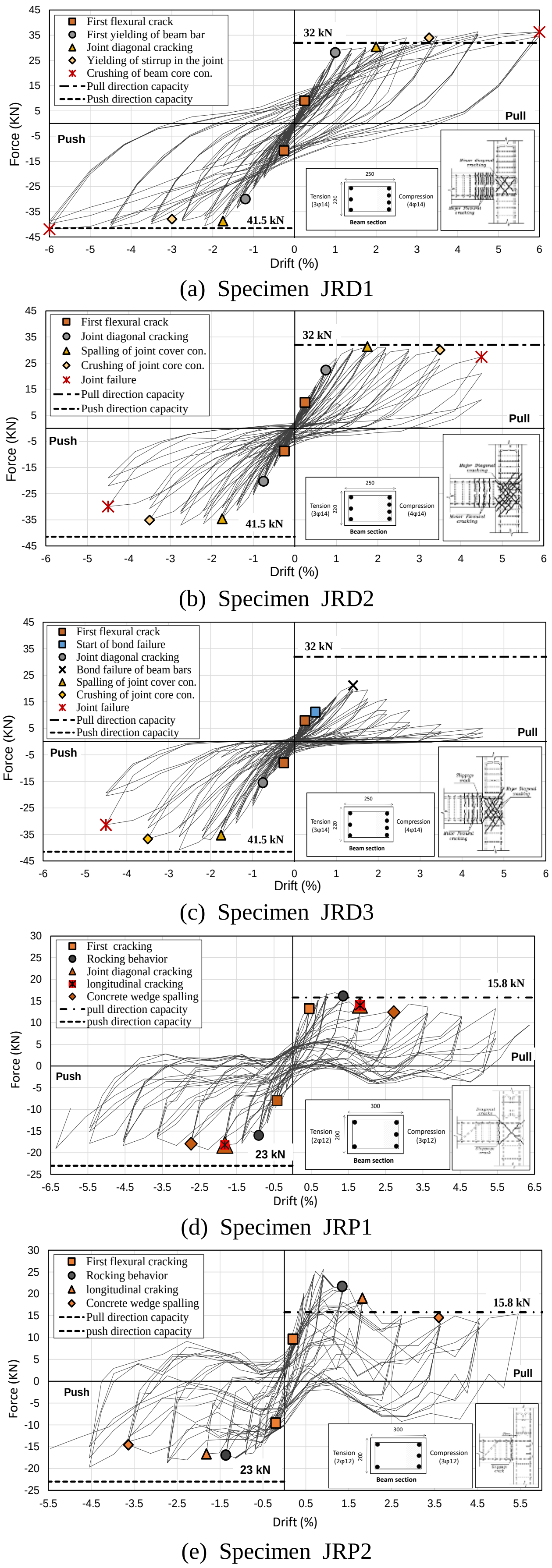

Fig. 15 Force–displacement hysteretic responses of Jo int specimens

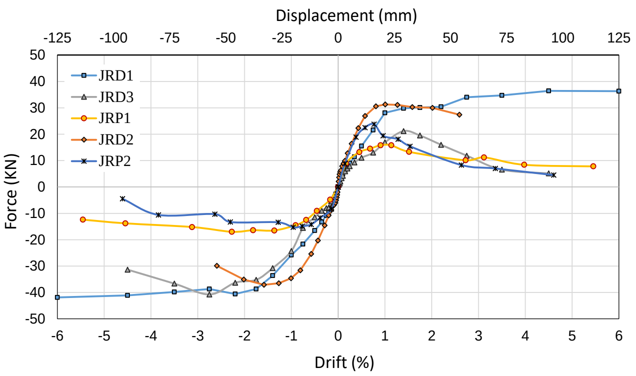

Fig. 16 Comparison of force–displacement envelope curves of the joint specimens

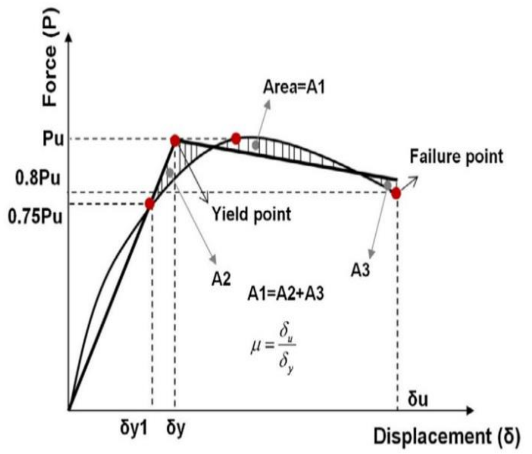

Fig. 17 Characteristic points on force–displacement cu rve

develop full nominal flexural strength like specimen JRP1. Overall, larger axial force in the column has raised flexural strength of the joint by an average rate of 25%.

As shown in Figs. 13, 14 and 15(e), the cracking mechanism of the JRP2 specimen is quite similar to the JRP1 specimen. In this substructure, the axial load is $0.15f_c'\times b\times h$, which is increased compared to the JRP1 specimen. This amount of axial load is exactly equal to the axial load of joint specimens reinforced by deformed bars. The higher axial load in this specimen has caused no diagonal cracking in the panel zone of the joint. In this specimen like the joint specimen JRP1, deep slippage crack at the face of the column is the main mechanism of cracking. However, the higher axial load caused the location of the crack shifted to out of the connection area in the beam.

4.2 Force–displacement envelope curves

The envelope curves of all specimens based on peak force are shown in Fig. 16. Using these envelope curves were obtained the peak load, ultimate displacements and ductility capacity for the specimens for positive and negative loading direction as reported in Table 4 and 5. Definition of yield displacement is necessary for calculating ductility capacity of substructures and it often causes difficulty because the force–displacement response of RC components may not have a well-defined yield point. This may occur, for example, due to nonlinear behavior of the materials (steel reinforcement and concrete) or due to yielding in different parts of a RC structure or sub-assemblage commencing at different load levels. Consequently, it has been general practice to define the ductility parameters of RC components based on an idealized bilinear force–displacement response. The value of ductility is obtained from the idealized bilinear response (Fig. 17) (Paulay and Priestley 1992, Park 1989, Priestley and Park 1987). Using the calculated yield and ultimate displacement, the ductility capacity value is determined by Eq. (1). The ultimate displacement, δ_u, is defined as the displacement corresponding to either a 20% drop of peak load, the buckling of longitudinal reinforcement, fracturing of longitudinal or transverse reinforcement (whichever occurs first) (Priestley and Paulay 1992).

Table 4 Developed strength of the specimens for positive and negative direction

Specimen	Peak load (KN)			Beam capacity (KN)			Peak load per capacity		
	Pull (+)	Push (-)	Average	Pull (+)	Push (-)	Average	Pull (+)	Push (-)	Average
JRD1	36.4	41.9	39.2	32	41.5	36.75	1.14	1.01	1.07
JRD2	31.3	37.1	34.2	32	41.5	36.75	0.98	0.89	0.93 (14%↓)
JRD3	21.1	36.3	28.7	32	41.5	36.75	0.66	0.87	0.78 (29%↓)
JRP1	16.9	19.3	18.1	15.8	23	19.4	1.07	0.84	0.93 (14%↓)
JRP2	25.6	17.6	21.6	15.8	23	19.4	1.62	0.77	1.11 (4%↑)

Table 5 Calculation of ductility for positive and negative direction

Specimen	Drift at yield point e_y(%)			Ultimate drift e_u(%)			Ductility factor m		
	Pull (+)	Push (-)	Average	Pull (+)	Push (-)	Average	Pull (+)	Push (-)	Average
JRD1	1.09	1.47	1.28	5.76	5.76	5.76	5.29	3.91	4.60
JRD2	1.15	1.47	1.31	4.32	4.32	4.32	3.75	2.93	3.34 (28%↓)
JRD3	1.22	1.73	1.47	2.06	4.32	3.19	1.70	2.50	2.10 (54%↓)
JRP1	0.49	0.97	0.73	2.72	2.72	2.72	5.55	2.80	4.18 (9%↓)
JRP2	0.57	0.60	0.59	3.64	3.64	3.64	6.39	6.07	6.23 (35%↑)

$$\mu=\frac{\delta_u}{\delta_y} \tag{1}$$

The results of Table 4 and Fig. 16 show that the ratio of the developed strength to the bearing capacity of the substructure in the joint specimens reinforced by deformed bars has reduced more than the joint specimens reinforced by plain bars.

In specimen JRD1, which is built up in accordance with the current seismic details, bearing capacity of the substructure has been developed in both of direction. In specimen JRD2, which has lack of transverse shear

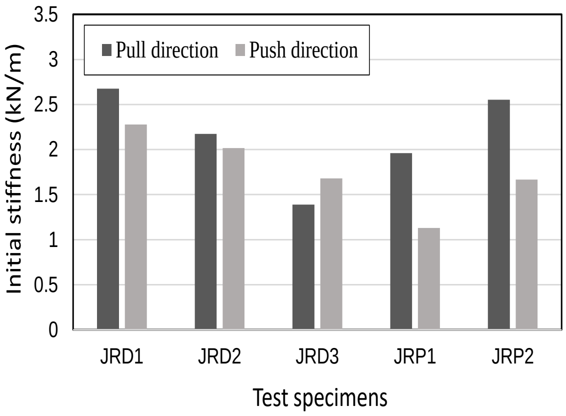

Fig. 18 Initial stiffness of the joint specimens

reinforcement in the panel zone of the joint, 93% of the average strength of the substructure is developed according to the Table 4. However, the average ductility of the substructure has decreased by 28% according to Table 5.

In specimen JRD3, which has lack of transverse shear reinforcement in addition to reducing development length of the longitudinal bars of the beam, the substructure has been able to achieve only 78% of the average strength. The ductility of the specimen has also greatly reduced by 54% due to the reducing development length of the longitudinal bars of the beam (Table 5).

In joint specimen JRP1 that reinforced by plain bars, and has no shear reinforcement in the connection area, the reduction of the strength is exactly equal to the specimen JRD2, But the ductility of the specimen JRP1 has been reduced only 9% that was less than the joint reinforced by deformed bars due to different behavior between concrete and plain bars. Table 5 shows that ductility ratio of JRP1 is as high as 4.18 which is larger than expected. This may be justified by relatively large and stable slip of longitudinal reinforcements of the beams, and stability of the response is attributed to hooks at the end of the bars.

In specimen JRP2, which has similar details to specimen JRP1 and has only increased axial load ($0.15f'c \times b \times h$), the strength of the substructure increases slightly (10%) due to the confinement of the joint by axial load of the column. The ductility of the joint specimen by higher axial load increased by 35%.

The results represented in Table 5 shows that there are meaningful points in the comparison of average ductility and peak load per capacity ratios of beam-column joints reinforced by deformed and plain bars. Varity of the ductility ratio clearly shows that application of the plain bars improved the ductility ratio of the specimens. Also, despite of expected reduction in the ratio of peak load per capacity of the beam-column joints reinforced by plain bars, it was shown that the joint specimen reinforced by plain bars have the same ratio of resistance per capacity due to use of 180° end hooks at the end of development length of the bars.

4.3 Stiffness degradation

One of the main parameters influencing the seismic behavior of the structural elements is the initial stiffness. The initial stiffnesses of the sub-structures reinforced by plain and deformed bars are shown in Fig. 18 and Table 6.

Table 6 Initial and reduction stiffness of the joint specimens

Specimen	Initial stiffness (kN/m)		Reduction of initial stiffness with regard to the seismic specimen JRD1 (%)		
	Pull (+)	Push (-)	Pull (+)	Push (-)	Average
JRD1	2.68	2.28	-	-	-
JRD2	2.17	2.02	18.79	11.46	15.12
JRD3	1.39	1.68	48.13	26.20	37.17
JRP1	1.96	1.13	26.78	50.35	38.57
JRP2	2.55	1.67	4.66	26.81	15.73

Seismic specimen JRD1 has the most stiffness in both directions of lateral loading. The initial stiffnesses in the specimens JRD2 and JRD3 representing the deficient joint specimens reinforced by deformed bars, are reduced by 15.12% and 37.17%, respectively with regard to the specimen JRD1.

As shown in Table 6, the initial stiffness of the joint specimen reinforced by plain bars (JRP1) is reduced more than joint specimen reinforced by deformed bars (JRD2) due to more sliding of the bars throughout the concrete. As described before, both of these joint specimens have not any shear reinforcement in the joint region. However, initial stiffness in joint specimen JRP2 is decreased less than joint specimen JRP1 due to the confinement of the joint by more axial load.

4.4 Strains in development length

Strain gages were installed on longitudinal bars of the beam and column and in the joint panel in order to measure local strains and compare with the yield strains. Yield strains of the reinforcements are presented in Table 3. The results are presented in Fig. 19.

The comparison of the strain distribution curves along the longitudinal bars in the joint specimens reinforced by plain and deformed bars shows that the tension of the longitudinal bars of the beam in the joint specimens reinforced by plain bars is not reduced until to the end of the bar and reaching to the end hook, however in the joint specimens reinforced by deformed bar, the reduction in the strain rate at the end of the bar is clearly evident. As it was seen in the experiment, cohesion of the bar to concrete in the structural element (beam) reinforced by plain bars was lost soon due to the occurrence of the debounding between bars and concrete, and it caused the force distributed along the longitudinal bars of the beam is not reduced until reaching to the hook at the end of the bar. In other way, the main factor in the transfer of the force of the rebar to the concrete is the end hook of the plain bar.

Also, longitudinal bars of the beam in the joint specimens reinforced by deformed bar (JRD2 and JRD3) reach to the yielding stress limit at the drift ratio of 1.1% and 2.2%, respectively. However, in the joint specimen reinforced by plain bars (JRP1), the longitudinal bars of the

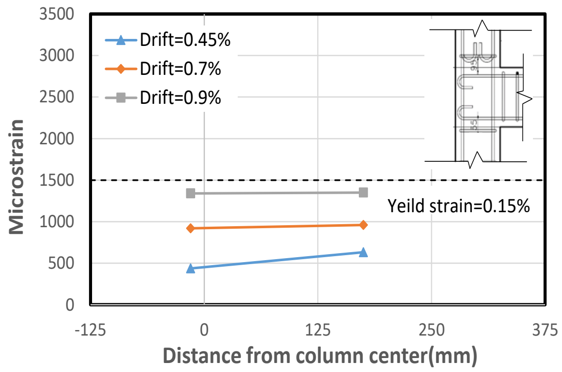

(a) Specimen JRP1

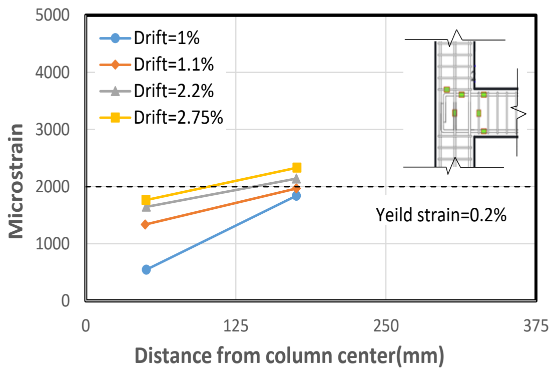

(b) Specimen JRD2

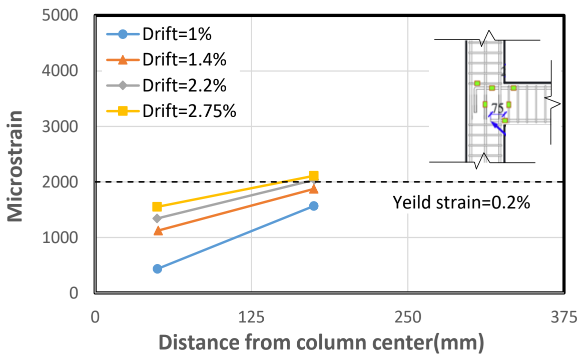

(c) Specimen JRD3

Fig. 19 Measured strains along bottom beam bar

beam reach to the yielding stress limit at the drift ratio of 1%. The strain-gages in specimen JRP1 reached 1250 μs ($0.85\varepsilon_y$) at a drift ratio of 0.9%. Such a relatively large strain may be explained by the effect of the end hook bar (180°) that has enabled such a strain magnitude to develop at such a relatively small drift ratio. The horizontal dashed lines in these figures shows the yield strain of longitudinal reinforcements.

4.5 Energy dissipation capacity

Energy dissipation capacity is one of the most important criteria for assessing the performance of a component in the structures subjected to simulate seismic loading.

The total energy dissipated by RC components consists of (i) energy dissipated by the steel reinforcement, (ii) energy dissipated by friction along existing cracks in concrete, and (iii) energy dissipated during the formation of new cracks (Al-Salloum *et al*. 2011). The area enclosed by a complete hysteretic loop at each cycle represents the cyclic energy dissipated by the specimen (Ei), and the cumulative hysteresis energy dissipation capacity is calculated through summation of areas under the force displacement hysteretic curves ($\sum E_i$) (Priestly and Macrase 1996), as shown in Fig. 20.

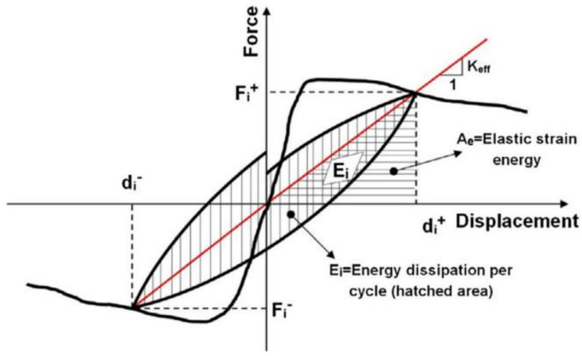

Fig. 20 Calculation of energy dissipation capacity of the substructures

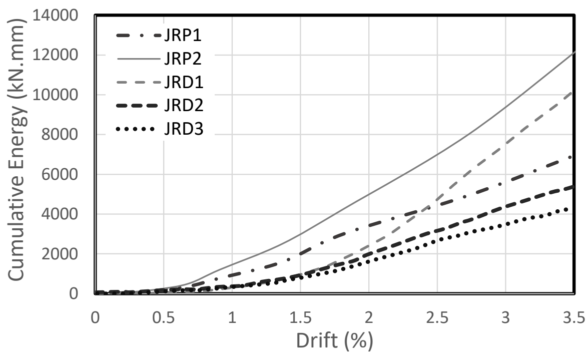

Fig. 21 Cumulative hysteresis energy dissipation for t he joint specimens

The cumulative energy dissipated by the experimental specimens versus drift ratio is shown in Fig. 21. As shown in Fig. 21, the energy dissipation of the joint specimens reinforced by plain bars is much larger than the joint specimens reinforced by deformed bars in the level of small drifts of the substructures. This is justified by relatively large and stable slip of longitudinal reinforcements of the beams, and stability of the response is attributed to hooks at the end of the bars. The rate of dissipation energy for specimens JRP1 and JRP2 are 940 kN and 1400 kN at the drift ratio of 1%, respectively. However, the energy dissipation in the specimen JRD1 is 320 kN at the represented drift ratio.

The situation in the level of lateral nonlinear drift ratio of the substructures is different and energy dissipation of seismic joint specimen reinforced by deformed bars (JRD1) is increasing exponentially by growing up the lateral drift ratio. But joint specimens JRD2 and JRD3 that represented deficient joints reinforced by deformed bars do not show significant increase in energy dissipation of the substructures due to lack of seismic reinforcement. The energy dissipated from the beginning of the test till ±3.5%

drift ratio for the joint specimens reinforced by deformed bars (specimens JRD1, JRD2 and JRD3) was 10.3, 5.3 and 4.3 kN.m, respectively.

In addition, in joint specimen reinforced by plain bars (JRP2), which undergoes much larger axial load than specimen JRP1, the energy dissipation increases due to more confinement of the joint (which is the focused damage region). The cumulative energy dissipated from the beginning of the test up to a drift ratio of ±3.5% for specimens JRP1 and JRP2 are 6.35 and 12.05 kN.m, respectively (Fig. 21).

5. Conclusions

Five half-scaled external beam–column joints reinforced by plain and deformed bars of existing concrete structures were tested and the behavior of the specimens were investigated and compared. Three units were tested as beam–column joints reinforced by deformed bars (specimens JRD1, JRD2, and JRD3), that one of them (specimen JRD1) represented a seismic beam–column joint designed to satisfy ACI 318M-11 requirements (2005). Two other units were tested as beam–column joints reinforced by plain bars (specimens JRP1, JRP2). The main deficiencies of these joint specimens were the absence of transverse steel hoops, the anchorage condition of longitudinal reinforcements. The units were tested under increasing lateral cyclic load in combination with constant axial load. The results of the experimental study can be summarized as follows:

- Specimen JRD1 which represented a seismic beam–column joint reinforced by deformed bars, failed by flexural yielding in the beam with moderately ductile performance and the cracking in the panel zone of the joint is insignificant.
- Using of plain bars caused to appear different damage modes in the joint specimens with the same deficiency. It caused shear strength of the joints by plain bar to be decreased compared to the joints by deformed bars. The main damage modes of the joint specimens which has lack of shear reinforcement are as follows:
- For the joint reinforced by plain bars is deep crack at the face of the column due to debounding and slippage of the bars throughout the concrete in the joint region.
- For the joint reinforced by deformed bars is developing major diagonal cracking in panel zone of the joint in addition to minor flexural cracking at the end of the beam.
- Reducing development length of the bars in joint reinforced by deformed bars caused to appear deep slippage crack at the face of the column like joint reinforced by plain bars.
- In joint specimens reinforced by plain bars, higher axial load of the column and more confinement of the panel zone caused to shift the deep sliding crack far from the column face and any diagonal cracking was not seen in the panel zone.
- The hysteretic loops of the non-seismic specimens show considerable pinching and continuous stiffness degradation with increasing displacement with respect to the seismic specimen, which was primarily attributed to the joint shear failure and bond failure of the beam bottom reinforcement of joint specimens.
- The ratio of the developed strength to the bearing capacity of the substructure in deficient joint specimens were decreased regarding to the seismic joint specimen. Truss mechanism for shear transferring in the represented deficient joints was not formed due to lack of shear reinforcement.
- Deficient joint specimen with lack of enough development length of longitudinal bars has the least bearing capacity of the substructure. Also, joint specimen reinforced by plain bars and confined by more axial load showed the most bearing capacity of the substructure. Observation of the test showed that using hook at the end of the plain longitudinal bars helps to form strut and tie mechanism for shear transferring more strongly.
- Varity of the ductility ratio clearly shows that application of the plain bars improved the ductility ratio of the joint specimens.
- The initial stiffness of the joint specimen reinforced by plain bars (JRP1) is reduced more than joint specimen reinforced by deformed bars (JRD2) due to more sliding of the bars throughout the concrete.
- The energy dissipation of the joint specimens reinforced by plain bars is much larger than the joint specimens reinforced by deformed bars in the level of small drifts of the substructures. This is justified by relatively large and stable slip of longitudinal reinforcements of the beams, and stability of the response is attributed to hooks at the end of the bars.

References

ACI 374.1-05 (2005), Acceptance Criteria for Moment Frames based on Structural Testing and Commentary, Michigan, U.S.A.

ACI Committee 318M-11 (2011), Building Code Requirements for Structural Concrete (aci 318m-11) and Commentary, American Concrete Institute; Farmington Hills, MI, U.S.A.

Adibi, M., Marefat, M.S., Arani, K.K. and Zare, H. (2017a), "External retrofit of beam-column joints in old fashioned rc structures", *Earthq. Struct*., **12**(2), 237-250. https://doi.org/10.12989/eas.2017.12.2.237.

Adibi, M., Marefat, M.S., Esmaeily, A., Arani, K.K. and Esmaeily, A. (2017b), "Seismic retrofit of external concrete beam-column joints reinforced by plain bars using steel angles prestressed by cross ties", *Eng. Struct. J*., **148**(1), 813-828. https://doi.org/10.1016/j.engstruct.2017.07.014.

Al-Salloum, Y.A., Almusallam, T.H., Alsayed, S.H. and Siddiqui, N.A. (2011), "Seismic behavior of as-built, ACI-complying, and CFRP-repaired exterior RC beam–column joints", *J. Compos. Constr*., **15**(4), 522-534. https://doi.org/10.1061/(ASCE)CC.1943-5614.0000186.

ATC (1989), Handbook for Seismic Evaluation of Existing Buildings ATC-22, Applied Technology Council, California, U.S.A.

Barker, J.A. (1979), *Reinforced Concrete Detailing*, Oxford University Press, London, U.K.

Bedirhanoglu, I., Ilki, A. and Kumbasar, N. (2013). "Precast fiber reinforced cementitious composites for seismic retrofit of deficient rc joints-a pilot study", *Eng. Struct.*, **52**, 192-206, https://doi.org/10.1016/j.engstruct.2013.02.020.

Bedirhanoglu, I., Ilki, A., Pujol, S. and Kumbasar, N. (2010), "Behavior of deficient joints with plain bars and low-strength concrete", *ACI Struct. J.*, **107**(3), 300-310.

Braga, F., Gigliotti, R. and Laterza, M. (2009), "R/C existing structures with smooth reinforcing bars: experimental behaviour of beam-column joints subject to cyclic lateral loads", *Open Constr. Build. Tech. J.*, **3**, 52-67. http://dx.doi.org/10.2174/1874836800903010052.

Calvi, G.M., Magenes, G. and Pampanin, S. (2002), "Relevance of beam-column joint damage and collapse in RC frame assessment", *J. Earthq. Eng.*, **6**(1), 75-100. https://doi.org/10.1142/S1363246902000693.

De Risi, M.T., Ricci, P., Verderame, G.M. and Manfredi, G. (2016), "Experimental assessment of unreinforced exterior beam - column joints with deformed bars", *Eng. Struct. J.*, **112**(1), 215-232. https://doi.org/10.1016/j.engstruct.2016.01.016.

Del Vecchio, C., Di Ludovico, M., Balsamo, A., Prota, A., Manfredi, G., & Dolce, M. (2014), "Experimental investigation of exterior RC beam-column joints retrofitted with FRP systems", *J. Compos. Constr.*, **18**(4). https://doi.org/10.1061/(ASCE)CC.1943-5614.0000459.

Doğangün, A. (2004), "Performance of reinforced concrete buildings during the May 1, 2003 Bingöl Earthquake in Turkey", *Eng. Struct. J.*, **26**(6), 841-856. https://doi.org/10.1016/j.engstruct.2004.02.005.

Duhman, C.W. (1953), *The Theory and Practice of Reinforced Concrete*, Mcgraw-Hill Book Company, New York City, U.S.A.

Edvard, N.J. and Tanner, J.L. (1996), *Theory and problems of Reinforced Concrete Design*, Schaum Publishing Co., New York City, U.S.A.

Engindeniz, M., Kahn, L.F. and Abdul-Hamid, Z. (2005), "Repair and strengthening of reinforced concrete beam-column joints: State of the art", *ACI Struct. J.*, **102**(2), 1.

Fernandes, C., Melo, J., Varum, H. and Costa, A. (2013), "Cyclic behavior of substandard reinforced concrete beam-column joints with plain bars", *ACI Struct. J.*, **110** (1).

Ghobarah, A., Saatcioglu, M. and Nistor, I. (2006), "The impact of the 26 December 2004 earthquake and tsunami on structures and infrastructure", *Eng. Struct. J.*, **28**(2), 312-326. https://doi.org/10.1016/j.engstruct.2005.09.028.

Gur, T., Pay, A., Ramirez, J.A., Sozen, M.A., Johnson, A.M., Irfanoglu, A. and Bobet, A. (2009), "Performance of school buildings in Turkey during the 1999 Düzce and the 2003 Bingöl earthquakes", *Earthq. Spectra. J.*, **25**(2), 239-256.

Hakuto, S. (1995), "Retrofitting of reinforced concrete moment resisting frames", Ph.D. Dissertation, University of Canterbury, Christchurch, New Zealand.

Hall, J.F., Holmes, W.T. and Somers, P. (1996), "Northridge earthquake of January 17, 1994: reconnaissance", Report Vol. 1, Earthquake Engineering Research Institute, California, U.S.A.

Kam, W.Y., Pampanin, S. and Elwood, K. (2011), "Seismic performance of reinforced concrete buildings in the 22 February Christchurch (Lyttleton) earthquake", *Bullt. NZ Soc. Earthq. Eng.*, **44**(4). http://hdl.handle.net/10092/9006.

Khan, M.I., Al-Osta, M.A., Ahmad, S. and Rahman, M.K. (2018), "Seismic behavior of beam-column joints strengthened with ultra-high performance fiber reinforced concrete", *Compos. Struct. J.*, **200**, 103-119. https://doi.org/10.1016/j.compstruct.2018.05.080.

Liu, A. and Park, R. (2000), "Seismic behavior of existing moment-resisting frames with plain round reinforcing bars designed to pre-1970s codes", *Proceeding of 12th World Conference on Earthquake Engineering*, Auckland, New Zealand, February.

Liu, A. and Park, R. (2001), "Seismic behaviour and retrofit of pre 1970's as built exterior beam-column joint reinforced by plain bars", *Bull. NZ. Soc. Earthq. Eng.*, **34**(1), 68-81. https://doi.org/10.5459/bnzsee.34.1.68-8.

Lowes, L. and Altoontash, A. (2003), "Modeling reinforced-concrete beam-column joints subjected to cyclic loading", *J. Struct. Eng.*, **129**(12), 1686-1697. https://doi.org/10.1061/(ASCE)0733-9445(2003)129:12(1686).

Masi, A., Santarsiero, G., Moroni, C., Nigro, D., Dolce, M., Russo, G. and Manfredi, G. (2008), "Behaviour and strengthening of RC beam-column joints", *The 14th World Conference on Earthquake Engineering*, Beijing, China, October.

Masi, A., Santarsiero, G., Verderame, G., Russo, G., Martinelli, E., Pauletta, M. and Cortesia, A. (2009), "Capacity models of beam-column joints: provisions of european and italian seismic codes and possible improvements", *Conference*, Reluis Italian National Research Project, Italy, April.

Miller, D.K. (1998), "Lessons learned from the Northridge earthquake", *Eng. Struct. J.*, **20**(4-6), 249-260. https://doi.org/10.1016/S0141-0296(97)00031-X.

Mo, Y.L. and Chan, J. (1996), "Bond and slip of plain rebars in concrete", *J. Mater. Civil Eng.*, **8**(4), 208-211. https://doi.org/10.1061/(ASCE)0899-1561(1996)8:4(208).

Moehle, J.P. and Mahin, S.A. (1991), "Observations on the behavior of reinforced concrete buildings during earthquakes, In: Ghosh SK, edito", ACI Publication SP-127, Earthquake-Resistant Concrete Structures, Inelastic Response and Design.

Pampanin, S., Calvi, G.M. and Moratti, M. (2002), "Seismic behaviour of R.C. beam-column joints designed for gravity loads", *Proceeding of 12th European Conference on Earthquake Engineering*, London, U.K, September.

Park, R. (1989), "Evaluation of ductility of structures and structural assemblages from laboratory testing", *Bull. NZ. Soc. Earthq. Eng.*, **22**(3), 155-166. https://doi.org/10.5459/bnzsee.22.3.155-166.

Park, R. and Paulay, T. (1975), *Reinforced Concrete Structures*, John Wiley and Sons Company, New Jersey, U.S.A.

Park, R., Billings, I.J., Clifton, G.C., Cousins, W.J., Filiatrault, A., Jennings, D.N., Jones, L.C.P., Perrin, N.D., Rooney, S.L., Sinclair, J., Spurr, D.D., Tanaka, H. and Walker, G. (1995), "The Hyogo-ken Nanbu Earthquake (The Great Hanshin Earthquake) of 17 January 1995", Report of the NZNSEE Reconnaissance Team, *Bull. NZ. Natl. Soc. Earthq. Eng.*, **28**(1), 1-98.

Paulay, T. and Priestley, M.J.N. (1992), *Seismic Design of Reinforced Concrete and Masonry Buildings*, John Wiley and Sons, Inc., New York, U.S.A.

Pernot, P. (1954), *Le Beton Arme*, J. B. Balliere et Fils, Editeurs, Paris, France.

Priestley, M.J.N. and MacRae, G.A(1996), "Seismic tests of precast beam-to-column joint subassemblages with unbonded tendons", *PCI. J.*, **41**(1), 64-81.

Priestley, M.J.N. and Park, R. (1987) "Strength and ductility of concrete bridge columns under seismic loading", *ACI Struct. J.*, **84**(1), 61-76.

Russo, G. and Pauletta, M. (2012), "Seismic behavior of exterior beam-column connections with plain bars and effects of upgrade", *ACI Struct. J.*, **109**(2), 225-233.

Sezen, H., Elwood, K.J., Whittaker, A.S., Mosalam, K.M., Wallace, J.W. and Stanton, J.F. (2000), "Structural engineering reconnaissance of the August 17, 1999 Kocaeli (Izmit), Turkey Earthquake", Technical Rep. No., PEER 2000, 9.

Sezen, H., Whittaker, A.S., Elwood, K.J. and Mosalam, K.M. (2003), "Performance of reinforced concrete buildings during the August 17, 1999 Kocaeli, Turkey earthquake, and seismic design and construction practice in Turkey", *Eng. Struct. J.*,

25(1), 103-114. https://doi.org/10.1016/S0141-0296(02)00121-9.

Shafaei, J., Zareian, M., Hosseini, A. and Marefat, M. (2014), "Effects of joint flexibility on lateral response of reinforced concrete frames", *Eng. Struct. J.*, **81**(15), 412-431. https://doi.org/10.1016/j.engstruct.2014.09.046.

Taylor, F.W., Thompson, S.E. and Smulski, E. (1925), *Concrete Plain and Reinforcement*, 4th Edition, John Wiley and Sons Company, New Jersey, U.S.A.

Tsonos, A.G. and Stylianidis, K. (2002), "Seismic retrofit of beam-to-column joints with high-strenght fiber jackets", *Eur. Earth. Eng.*, **16**(2), 56-72.

Uang, C.M., Elgamal, A., Li, W.S. and Chou, C.C. (1999), "Ji-Ji, Taiwan earthquake of September 21, 1999", A Brief Reconnaissance Report, San Diego, Department of Structural Engineering, University of California, U.S.A.

Verderame, G.M., De Carlo, G., Ricci, P. and Fabbrocino, G. (2009), "Cyclic bond behaviour of plain bars. Part II: Analytical investigation", *Constr. Build. Mater.*, **23**(12), 3512-3522. https://doi.org/10.1016/j.conbuildmat.2009.07.001

Xing, G., Zhou, C., Wu, T. and Liu, B. (2015), "Experimental study on bond behavior between plain reinforcing bars and concrete", *Adv. Mater. Sci. Eng. J.*, **2015**. https://doi.org/10.1155/2015/604280.

Youssef, M. and Ghobarah, A. (2001), "Modelling of RC beam-column joints and structural walls", *J. Earthq. Eng.*, **5**(1), 93-111. https://doi.org/10.1142/S1363246901000303.

Zhao, B., Taucer, F. and Rossetto, T. (2009), "Field investigation on the performance of building structures during the 12 May 2008 Wenchuan earthquake in China", *Eng. Struct. J.*, **31**(8), 1707-1723. https://doi.org/10.1016/j.engstruct.2009.02.039.

CC